Available online at www.sciencedirect.com

SCIENCE DIRECT®

Journal of Organometallic Chemistry 679 (2003) 116–124

Journal of Organo metallic Chemistry

www.elsevier.com/locate/jorganchem

Transition metal (Group 6, Ru and Group 10) derivatives of aminophosphines, $Ph_2PN(H)R$ (R = Ph, C_6H_{11})

Srinivasan Priya [a], Maravanji S. Balakrishna [a,*], Joel T. Mague [b]

[a] Department of Chemistry, Indian Institute of Technology, Bombay, Powai, Mumbai 400 076, India
[b] Department of Chemistry, Tulane University, New Orleans, LA 70118, USA

Received 3 June 2003; received in revised form 6 June 2003; accepted 6 June 2003

Abstract

The reactions of aminophosphines with Group 6 metal carbonyls afford both mono-substituted and disubstituted complexes. The reaction of $Ph_2PN(H)C_6H_{11}$ with molybdenum tetracarbonyl derivative gives a mixture of *cis* and *trans*-isomers. The reaction of $Ph_2PN(H)Ph$ with $Pd(COD)Cl_2$ leads to the P–N bond cleavage to give chloro bridged dimer, $[Pd(PPh_2O)(PPh_2OH)(\mu\text{-}Cl)]_2$, whereas with $Pt(COD)Cl_2$, disubstituted *cis*-$[PtCl_2\{PPh_2N(H)R\}_2]_2$ was obtained. The reaction of $Ph_2PN(H)C_6H_{11}$ with $RuCl_2(DMSO)_4$ or $RuCl_2(PPh_3)_3$ leads to the formation of ionic complex, $[RuCl\{Ph_2PN(H)C_6H_{11}\}_3]Cl$.

Keywords: Aminophosphine; Transition metal complexes; Metalloligands; P–N bond; Cleavage; *Trans*-isomer

1. Introduction

The transition metal chemistry of aminobis(phosphines), $X_2PN(R)PX_2$ [1] is well documented whereas that of the corresponding aminophosphines, $X_2PN(H)R$ is limited [2]. This is partly due to the sensitivity of the P(III)–N bonds towards acid or base catalysed hydro lysis during complexation reactions [3]. However, by choosing appropriate substitutents on both phosphorus and nitrogen centers P(III)–N bonds can be even stabilized towards lithium reagents [4]. The intramolecular donor–acceptor properties of aminophosphines with a ferrocene backbone confirm that the aminophosphines can stabilize the transition metals in both high-valent (Ti group metals) and low-valent states (platinum metals) and also they can act as both terminal and bridging ligands [5]. The phosphinoamide complex, $[Zr\{N(Ph)PPh_2\}_4]$ is found to be an active catalyst for the formation of elastomeric polypropylene in the presence of methylaluminoxane [6]. Recently we have reported on insertions of carbon fragments into the P(III)–N bonds in aminophosphines and aminobis(phosphines) and also the cleavage of P(III)–N bonds in the reactions with aldehydes [7]. As a part of our interest on aminophosphines [8] and of others [2c,9], we report here the synthesis and structural investigations of aminophosphines with transition metal derivatives.

2. Experimental

All manipulations were performed under anaerobic conditions using Schlenk techniques. The ligands, $Ph_2PN(H)R$ (R = Ph, [10] C_6H_{11} [7]), and the metal precursors $M(COD)Cl_2$ (M = Pd [11], Pt [12]) $RuCl_2(PPh_3)_3$ [13], $RuCl_2(DMSO)_4$ [14], $M(CO)_4(NBD)$ (M = Mo [15], Cr [16]) and $W(CO)_4(pip)_2$ [17], were prepared according to the literature procedures. $Ni(CO)_2(PPh_3)_2$ was purchased from Strem Chemical Co. The ^1H and ^{31}P-NMR spectra were recorded using Varian VXR 300 and Bruker AMX 400 spectrometers operating at the appropriate frequencies using tetramethylsilane and 85% H_3PO_4 as internal and external references, respectively. Positive shifts lie downfield in all cases. IR spectra were recorded on a Nicolet Impact

---

* Corresponding author. Fax: +91-22-2576-7152.
E-mail address: krishna@iitb.ac.in (M.S. Balakrishna).

0022-328X/03/$ - see front matter © 2003 Elsevier B.V. All rights reserved.
doi:10.1016/S0022-328X(03)00543-6

400 FT IR instrument in KBr matrix. Microanalyses were performed on a Carlo Erba model 1112 elemental analyser. The FAB mass spectra were recorded on JEOL SX 102/DA-6000 mass spectrometer/Data system using Argon/Xenon (6 kV, 10 mA) as FAB gas and high resolution mass spectra (HRMS) on MASCPEC (msco/9849) system. Melting points were determined in capillary tubes and are uncorrected.

2.1. Synthesis of $Cr(CO)_4\{PPh_2N(H)R\}_2$ (R = Ph, **3**; C_6H_{11}, **4**)

A mixture of $[Cr(CO)_4(NBD)]$ (0.04 g, 0.156 mmol) and $Ph_2PN(H)R$ (0.312 mmol) in *n*-hexane (10 ml) was heated to reflux for 12 h. The reaction mixture was cooled to room temperature (r.t.) and the yellow residue was separated by filtration, washed with *n*-hexane (3 × 5 ml) and recrystallized from CH_2Cl_2–*n*-hexane (2:1) mixture at 0 °C to get crystalline product of analytical purity.

2.2. $Cr(CO)_4\{PPh_2N(H)Ph\}_2$ (**3**)

Yield: 0.056 g (50%). M.p. 175–177 °C (dec.). Anal. Calc. for $C_{40}H_{32}N_2O_4P_2Cr$: C 66.85; H 4.49; N 3.89%. Found: C 66.51; H 4.56; N 3.79%. FTIR (KBr cm^{-1}): ν(NH) 3389s; ν(CO) 2009vs, 1917vs, 1901vs, 1887vs. ^1H-NMR ($CDCl_3$): δ 7.92–7.00 (m, PPh, 10H), 6.66 (t, N-Ph-*m*, 2H), 6.50 (t, N-Ph-*p*, 1H), 5.95 (br s, N-Ph-*o*, 2H), 4.32 (br s, N*H*, 1H). $^{31}P\{H\}$-NMR ($CDCl_3$): δ 89.9 (s).

2.3. $Cr(CO)_4\{PPh_2N(H)C_6H_{11}\}_2$ (**4**)

Yield: 0.042 g (46%). M.p. 177–180 °C (dec.). Anal. Calc. for $C_{40}H_{44}N_2O_4P_2Cr$: C 65.75; H 6.07; N 3.83%. Found: C 65.15; H 6.19; N 3.76%. FTIR (KBr cm^{-1}): ν(NH) 3399s; ν(CO) 2009vs, 1912vs, 1892vs, 1846s. ^1H-NMR ($CDCl_3$): δ 8.07–7.05 (m, *phenyl*, 10H), 2.09–0.78 (m, *cyclohexyl*, 11H). $^{31}P\{H\}$-NMR ($CDCl_3$): δ 94.4 (s).

2.4. Synthesis of $Mo(CO)_4\{PPh_2N(H)Ph\}_2$ (**5**)

A mixture of $Mo(CO)_4(NBD)$ (0.050 g, 0.166 mmol) and $Ph_2PN(H)Ph$ (0.092 g, 0.333 mmol) in heptane (10 ml) was refluxed for 2 h. The red–brown solution obtained was evaporated to dryness and dissolved in CH_2Cl_2–*n*-hexane (1:3) mixture and kept at r.t. for 2 h to give pale-yellow crystalline product **5**. Yield: 0.051 g (40%). M.p. 139–142 °C (dec.). Anal. Calc. for $C_{40}H_{32}N_2O_4P_2Mo$: C 63.00; H 4.23; N 3.67%. Found: C 63.18; H 4.26; N 3.43%. FTIR (KBr cm^{-1}): ν(NH) 3385s; ν(CO) 2019s, 1939vs, 1926vs, 1892vs. ^1H-NMR (CD_2Cl_2): δ 7.65–7.38 (m, P*Ph*, 20H), 6.82 (t, N-Ph-*m*, 4H, $^3J_{HH} = 7.5$ Hz), 6.63 (t, N-Ph-*p*, 1*H*, $^3J_{HH} = 7.5$ Hz), 6.05 (d, N-Ph-*o*, 2H, $^3J_{HH} = 7.5$ Hz), 4.20 (br, N*H*, 2H). $^{31}P\{H\}$-NMR (CD_2Cl_2): δ 69.8 (s).

2.5. Synthesis of *cis*-$[Mo(CO)_4\{PPh_2N(H)C_6H_{11}\}_2]$ (**6**)

A mixture of $Mo(CO)_4(HNC_5H_{10})_2$ (0.050 g, 0.130 mmol) and $Ph_2PN(H)C_6H_{11}$ (0.075 g, 0.264 mmol) in CH_2Cl_2 (10 ml) was stirred at r.t. for 8 h. The solvent was evaporated from the reaction mixture under reduced pressure and the residue was washed with *n*-hexane (3 × 5 ml) and was re-crystallized from CH_2Cl_2–*n*-hexane (1:3) mixture and kept at 0 °C to give analytically pure sample of **6**. Yield: 0.081 g (80%). M.p. 136–139 °C (dec.). Anal. Calc. for $C_{40}H_{44}N_2O_4P_2Mo$: C 62.02; H 5.72; N 3.62%. Found: C 62.17; H 5.63; N 3.56%. FTIR (KBr cm^{-1}): ν(NH) 3399s; ν(CO) 2014s, 1928vs, 1913vs, 1882vs. ^1H-NMR ($CDCl_3$): δ 7.61–7.36 (m, *phenyl*, 10H), 2.47–0.88 (m, *cyclohexyl*, 11H). $^{31}P\{H\}$-NMR ($CDCl_3$): δ 74.5 (s).

2.6. Synthesis of $W(CO)_4\{PPh_2N(H)R\}_2$ (R = Ph, **7**; C_6H_{11}, **8**)

A mixture of $[W(CO)_4(NHC_5H_{10})_2]$ (0.05 g, 0.107 mmol) and $Ph_2PN(H)R$ (0.210 mmol) in CH_2Cl_2 (10 ml) was stirred at r.t. for 8 h. The reaction mixture was evaporated under reduced pressure and the residue obtained was washed with *n*-hexane (5 × 5 ml) and re-crystallized from CH_2Cl_2–*n*-hexane (2:1) mixture at 0 °C.

2.7. $W(CO)_4\{PPh_2N(H)Ph\}_2$ (**7**)

Yield: 0.083 g (91%). M.p. 141–144 °C (dec.). Anal. Calc. for $C_{40}H_{32}N_2O_4P_2W$: C 56.49; H 3.79; N 3.30%. Found: C 56.64; H 3.70; N 3.38%. FTIR (KBr cm^{-1}): ν(NH) 3394s; ν(CO) 2014s, 1922s, 1893vs, 1880vs. ^1H-NMR ($CDCl_3$): δ 7.67–7.25 (m, P*Ph*, 10H), 6.84 (t, N-Ph-*m*, 2H, $^3J_{HH} = 8.1$ Hz), 6.65 (t, N-Ph-*p*, 1*H*, $^3J_{HH} = 7.7$ Hz), 6.02 (d, N-Ph-*o*, 2H, $^3J_{HH} = 7.6$ Hz), 4.37 (br s, N*H*, 1H). $^{31}P\{H\}$-NMR ($CDCl_3$): δ 50.7 ($^1J_{WP} = 253.1$ Hz).

2.8. $W(CO)_4\{PPh_2N(H)C_6H_{11}\}_2$ (**8**)

Yield: 0.071 g, (70%). M.p. 129–132 °C (dec.). Anal. Calc. for $C_{40}H_{44}N_2O_4PW \cdot CH_2Cl_2$: C 53.73; H 5.06; N 3.05%. Found: C 53.77; H 4.91; N 3.04%. FTIR (KBr cm^{-1}): ν(NH) 3384s; ν(CO) 2014vs, 1912vs, 1872vs, 1826vs. ^1H-NMR ($CDCl_3$): δ 7.83–7.18 (m, *phenyl*, 10H), 3.03–0.45 (m, C_5H_{10} and *cyclohexyl*, 21H). $^{31}P\{H\}$-NMR ($CDCl_3$): δ 67.5 ($^1J_{WP} = 259.8$ Hz).

2.9. Synthesis of $Mo(CO)_5\{PPh_2N(H)Ph\}$ (**9**)

A mixture of $Mo(CO)_6$ (0.050 g, 0.189 mmol) and $Ph_2PN(H)Ph$ (0.053 g, 0.189 mmol) in benzene (10 ml) and the reaction mixture was heated at reflux for 12 h. The solvent was evaporated under reduced pressure and the residue obtained was extracted with *n*-hexane (3 × 7 ml) and the solution was passed through celite and the yellow filtrate was concentrated to 4 ml and cooled to give crystalline product of **5** in 21% yield (0.030 g).

The pale-yellow mother liquor on further concentration and cooling gave the crystalline product **9**. Yield: 0.035 g (36%). M.p. 120–124 °C (dec.). Anal. Calc. for $C_{23}H_{16}NO_5PMo$: C 53.82; H 3.14; N 2.73%. Found: C 53.57; H 3.12; N 2.67%. FTIR (ν cm^{-1}): ν(NH) 3414s; ν(CO) 2076s, 1986vs, 1906vs. ^1H-NMR ($CDCl_3$): δ 7.72–7.36 (m, P*Ph*, 10H), 7.04 (t, N-Ph-*m*, 2H, $^3J_{HH} = 7.68$ Hz), 6.82 (t, N-Ph-*p*, 1H, $^3J_{HH} = 7.32$ Hz), 6.60 (d, N-Ph-*o*, 2H, $^3J_{HH} = 7.71$ Hz), 4.18 (br s, NH, 1H). $^{31}P\{H\}$-NMR ($CDCl_3$): δ 73.0 (s). HRMS: 513.27 [M^+].

2.10. Synthesis of *trans*-$[Mo(CO)_4\{PPh_2N(H)C_6H_{11}\}_2]$ (**10**)

A mixture of $Mo(CO)_6$ (0.050 g, 0.189 mmol) and $Ph_2PN(H)C_6H_{11}$ (0.054 g, 0.189 mmol) in benzene (10 ml) was refluxed for 10 h. The solution was evaporated to dryness under reduced pressure and the residue obtained was dissolved in *n*-hexane (10 ml), passed through celite and the yellow filtrate was concentrated to 4 ml and cooled to 0 °C to give bright yellow crystals of **10**. Yield: 0.045 g (29%). M.p. 152–156 °C (dec.). Anal. Calc. for $C_{40}H_{44}N_2O_4P_2Mo$: C 62.02; H 5.72; N 3.61%. Found: C 61.91; H 5.72; N 3.66%. FTIR (KBr cm^{-1}): ν(NH) 3391s; ν(CO) 1884vs. ^1H-NMR ($CDCl_3$): δ 7.72–7.34 (m, *phenyl*, 10H), 2.69–0.76 (m, *cyclohexyl*, 11H). $^{31}P\{H\}$-NMR ($CDCl_3$): δ 85.2 (s).

The mother liquor on concentration and cooling to 0 °C gave pale yellow crystalline product of **6** in 20% (0.020 g) yield.

2.11. Synthesis of $[RuCl\{PPh_2N(H)C_6H_{11}\}_3]Cl$ (**11**)

$Ph_2PN(H)C_6H_{11}$ (0.094 g, 0.330 mmol) in CH_2Cl_2 (5 ml) was added to a solution of $RuCl_2(DMSO)_4$ or $RuCl_2(PPh_3)_3$ (0.080 mmol) in CH_2Cl_2 (7 ml) at r.t. The orange red reaction mixture was stirred at r.t. for 6 h. The solvent was evaporated under reduced pressure to give a sticky oil which was washed with *n*-hexane (2 × 5 ml) and the residue obtained was crystallized from CH_2Cl_2–*n*-hexane (2:1) mixture at 0 °C to give an analytically pure sample of 11. Yield: 0.079 g (80% with $RuCl_2(DMSO)_4$); 0.037 g (76% with $RuCl_2(PPh_3)_3$). M.p. 164–166 °C (dec.). Anal. Calc. for $C_{54}H_{66}N_3P_3RuCl_2 \cdot 2CH_2Cl_2$: C 56.43; H 5.92; N 3.53%. Found: C 56.23; H 5.81; N 3.37%. FTIR (KBr cm^{-1}): ν(NH) 3399 s. ^1H-NMR ($CDCl_3$): δ 8.07–7.05 (m, *phenyl*, 10H), 2.09–2.04 (br m. C*H*, 1H,), 1.92–0.78 (m, *cyclohexyl*, 10H). $^{31}P\{H\}$-NMR ($CDCl_3$): δ 76.4 (s). MS (FAB): 986 [M^+].

2.12. Synthesis of $[Pd(PPh_2O)(PPh_2OH)(\mu\text{-}Cl)]_2$ (**12**)

A solution of $Pd(COD)Cl_2$ (0.030 g, 0.105 mmol) in CH_2Cl_2 (5 ml) was added dropwise to $Ph_2PN(H)Ph$ (0.058 g, 0210 mmol) also in CH_2Cl_2 (4 ml) at r.t. The resultant clear solution was stirred at r.t. for 2 h to give turbid pale yellow solution. The reaction mixture was filtered and the filtrate was evaporated under reduced pressure and the residue obtained was washed with *n*-hexane (3 × 5 ml) and crystallized from CH_2Cl_2–*n*-hexane (2:1) mixture at 0 °C to give the product **12**. Yield: 0.038 g (73%). M.p. 187–190 °C (dec.). Anal. Calc. for $C_{48}H_{42}Cl_2O_4P_4Pd_2$: C 52.87; H 3.88%. Found: C 52.76; H 3.86%. ^1H-NMR ($CDCl_3$): δ 7.58–7.22 (m, *phenyl*). $^{31}P\{H\}$-NMR ($CDCl_3$): δ 79.0 (s).

The reaction of $Ph_2PN(H)Ph$ (0.068 g, 0.250 mmol) with K_2PdCl_4 (0.040 g, 0.120 mmol) in CH_3CN (7 ml) at r.t. for 6 h also yielded the product 12 (0.020 g, 33%).

2.13. Synthesis of $[Pt\{(PPh_2O)_2H\}_2]$ (**13**)

A solution of $Ph_2PN(H)Ph$ (0.040 g, 0.140 mmol) in CH_3CN (5 ml) was added to K_2PtCl_4 (0.030 g 0.072 mmol) in CH_3CN (5 ml) and the clear solution obtained was refluxed for 2 h, which resulted in the white suspension. The reaction mixture was filtered and the white residue was washed with CH_2Cl_2 (2 × 5 ml) and dried under vacuum and was identified as the complex **13**. Yield: 0.025 g (35%). M.p. 249–252 °C (dec.). Anal. Calc. for $C_{48}H_{42}O_4P_4Pt$: C: 57.55; H 4.23%. Found C: 57.22; H: 4.32%. ^1H-NMR (DMSO-d_6): δ 7.79–7.27 (m, *phenyl*). $^{31}P\{H\}$-NMR (DMSO-d_6): δ 53.4 ($^1J_{PtP} = 3958$ Hz).

2.14. Synthesis of $PtCl_2\{PPh_2N(H)R\}_2$ (R = Ph, **14**; C_6H_{11}, **15**)

A mixture of *cis*-$[PtCl_2(COD)]$ (0.030 g, 0.08 mmol) and $Ph_2PN(H)R$ (0.16 mmol) in CH_2Cl_2 (5 ml) was stirred for 6 h at r.t. The solvent was evaporated under reduced pressure to give a sticky residue, which was washed with *n*-hexane (2 × 5 ml) and dissolved in a mixture of CH_2Cl_2–*n*-hexane (3:1) and cooled to 0 °C to give analytically pure crystalline product.

2.15. $PtCl_2\{PPh_2N(H)Ph\}_2$ (**14**)

Yield: 0.044 g (67%). M.p. 217–220 °C (dec.). Anal. Calc. for $C_{36}H_{32}N_2Cl_2P_2Pt$: C 52.69; H 3.93; N 3.41%.

Found: C 52.65; H 3.89; N 3.39%. FTIR (KBr cm^{-1}): ν(NH) 3259 br.s. ^{1}H-NMR (CDCl$_3$): δ 7.58–7.21 (m, P*Ph*, 10H), 6.88 (t, N-Ph-*m*, 2H, $^3J_{HH} = 7.5$ Hz), 6.75 (t, N-Ph-*p*, 1H, $^3J_{HH} = 7.2$ Hz), 6.19 (d, N-Ph-*o*, 2H, $^3J_{HH} = 7.5$ Hz). ^{31}P{H}-NMR (CDCl$_3$): δ 28.8 ($^1J_{PtP} = 3927$ Hz).

2.16. $PtCl_2\{PPh_2N(H)C_6H_{11}\}_2$ (**15**)

Yield: 0.059 g (81%). M.p. 182–185 °C (dec.). Anal. Calc. for $C_{36}H_{44}N_2Cl_2P_2Pt \cdot CH_2Cl_2$: C 48.43; H 5.05; N 3.05%. Found: C 48.02; H 5.07; N 3.05%. FTIR (KBr cm^{-1}): ν(NH) 3245 br s. ^{1}H-NMR (CDCl$_3$): δ 7.61–7.23 (m, P*Ph*, 10H), 4.01 (br m, N*H*, 1H), 1.43–0.77 (m. *cyclohexyl*, 11H). ^{31}P{H}-NMR (CDCl$_3$): δ 29.6 ($^1J_{PtP} = 3951$ Hz).

2.17. Synthesis of $Ni(CO)_2\{PPh_2N(H)C_6H_{11})\}_2$ (**16**)

A mixture of $Ni(CO)_2(PPh_3)_2$ (0.050 g, 0.078 mmol) and $Ph_2PN(H)C_6H_{11}$ (0.044 g, 0.156 mmol) in CH_2Cl_2 (10 ml) was stirred at r.t. for 12 h. The solution was evaporated under reduced pressure and the residue obtained was washed with hot *n*-hexane (3 × 5 ml) to give analytically pure sample of **16**. Yield: 0.040 g (68%). M.p. 179–181 °C (dec.). Anal. Calc. for $C_{38}H_{44}N_2O_2P_2Ni \cdot CH_2Cl_2$: C: 61.12; H: 6.05; N: 3.66%. Found: C: 60.97; H: 6.06; N: 3.47%. FTIR (KBr cm^{-1}): ν(NH) 3128vs; ν(CO) 1997s; 1935s. ^{1}H-NMR (CDCl$_3$): δ 7.93–7.26 (m, *phenyl*, 10H), 2.99–1.16 (m. *cyclohexyl*, 11H). ^{31}P{H}-NMR (CDCl$_3$): δ 22.2 (s).

2.18. X-ray crystallography

Crystals of compounds **7**, **10**, **12** and **14** were mounted on Pyrex filaments with epoxy resin. Enraf-Nonius CAD-4 diffractometer was used for the unit cell determination and intensity data collection. The initially obtained unit cell parameters were refined by accurately centering randomly selected reflections in the 2θ ranges given in Table 1 (for **12** in Section 5). General procedures for crystal alignment and collection of intensity data on the Enraf-Nonius CAD-4 diffractometer have been published [18]. Periodic monitoring of check reflections showed stability of the intensity data. Details of the crystal and data collection are given in the Table 1. The data were corrected for Lorentz and polarization effects [19]. The calculations were performed with the SHELXTL PLUS [20] program package. The non-hydrogen atoms were geometrically fixed and allowed to refine using riding model and an empirical psi scan absorption correction was employed [21].

Table 1
Crystallographic data for compounds **7**, **10** and **14**

	7	**10**	**14**
Empirical formula	$C_{40}H_{32}N_2$-O_4P_2W	$C_{40}H_{44}Mo$-$N_2O_4P_2$	$C_{36}H_{32}Cl$-$2N_2P_2Pt$
Formula weight	862.56	774.65	820.57
Crystal system	Triclinic	Orthorhombic	Monoclinic
Space group	$P\bar{1}$ (No. 2)	*Pbca* (No. 61)	$P2_1$(No. 4)
a (Å)	14.927(2)	16.681(3)	11.315(3)
b (Å)	15.252(2)	10.111(1)	14.378(4)
c (Å)	18.530(3)	22.075(4)	20.402(5)
α (°)	79.433(2)	–	–
β (°)	67.885(2)	–	97.604(4)
γ (°)	86.155(2)	–	–
V (Å^3)	3842.0(10)	3723.4(11)	3290.0(15)
Z	2	4	4
D(calc.) (mg m^{-3})	1.500	1.382	1.653
λ(Mo–K$_\alpha$) [a] (Å)	0.71073	0.71073	0.71073
μ (Mo–K$_\alpha$) (mm^{-1})	3.1	0.5	4.6
Temperature (K)	100	−173	100
θ min–max (°)	1.2–28.3	1.9–28.3	1.7–28.3
R [b]	0.0259	0.0551	0.0429
WR	0.0821	0.1224	0.1111
a, b	0.0478, 7.5288	0.0384, 8.6238	0.0517, 19.4233

[a] Graphite monochromated.

[b] $w = 1/[\sigma^2(F_o)^2 + (aP)^2 + bP]$; $P = 1/3[F_o^2 + 2F_c^2]$.

3. Results and discussion

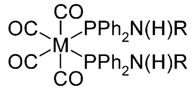

M = Cr, R = Ph, **3**; C_6H_{11}, **4**
M = Mo, R = Ph, **5**; C_6H_{11}, **6**
M = W, R = Ph, **7**; C_6H_{11}, **8**

The mononuclear metal carbonyl derivatives, *cis*-[$M(CO)_4\{PPh_2N(H)R\}_2$] (M = Cr, R = Ph, **3**; C_6H_{11}, **4**, M = Mo, R = Ph, **5**; C_6H_{11}, **6**, M = W, R = Ph, **7**; C_6H_{11}, **8**) were obtained by the displacement of either olefins or piperidine from the tetra carbonyl derivatives. The IR spectra of all the complexes, [$M(CO)_4L_2$] exhibit four bands in the carbonyl region (1885–2020 cm^{-1}) characteristic of the presence of *cis*-[$M(CO)_4$] with C_{2v} symmetry. The ^{31}P-NMR spectra of all the above complexes exhibit single resonances, which are deshielded from the corresponding free ligands. The coordination chemical shift value decreases considerably from chromium to tungsten as expected. The structure of complex *cis*-[$W(CO)_4\{PPh_2N(H)Ph\}_2$] is established by single crystal X-ray diffraction studies. The ORTEP [22] diagram of complex **7** is shown in Fig. 1 and the crystallographic data, selected bond distances and angles are listed in Tables 1 and 2. There are two molecules in the asymmetric unit but the corresponding bond distances and angles are not the same as shown in

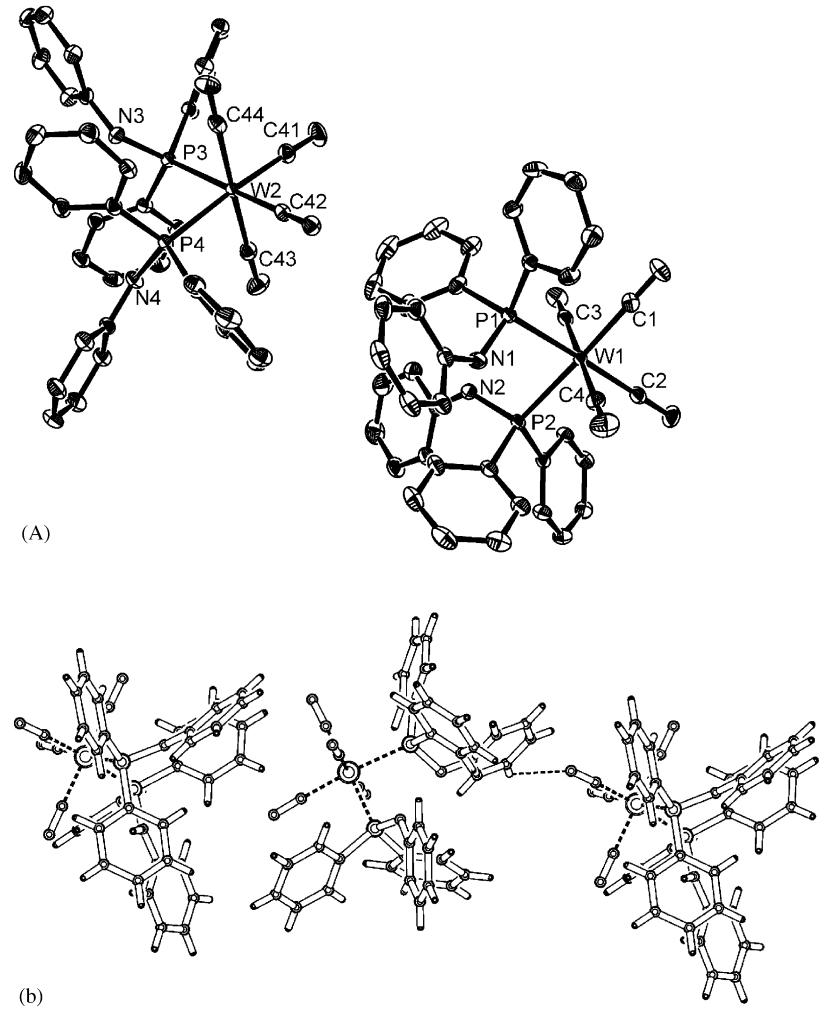

Fig. 1. (a) Perspective view of complex **7** drawn on 50% probability level. Hydrogen atoms are omitted for clarity. (b) Intermolecular C–H···OH bonding interaction.

Table 2. The tungsten atom is in a distorted octahedral environment and the bond angles around tungsten varies from 174.6(1)° to 177.4(1)°. The P–N bond distance (1.692(3) Å) is shorter than the Pauling scale due to the P–N multiple bonding. The W–P and W–C bond distances are 2.488(1)–2.499(1) Å and 2.001(3)–2.041(3) Å, respectively. In the lattice complex **7** shows intermolecular hydrogen-bonding interactions through phenyl hydrogens and the carbonyl oxygen atoms ($d_{C(59)\cdots O(2)} = 3.186(4)$ Å, $d_{H(59)\cdots O(2)} = 2.5856$ Å, C(59)–H(59)···O(2) bond angle = 121.47°) as shown in Fig. 1(b).

The reaction of **1** with equimolar quantity of $Mo(CO)_6$ in benzene yielded a mixture of mono-substituted complex, $Mo(CO)_5\{PPh_2N(H)Ph\}$ (**9**) and the disubstituted complex *cis*-$[Mo(CO)_4\{PPh_2N(H)Ph\}_2]$ (**5**) which were separated by fractional crystallization. The ^{31}P-NMR spectrum of complex **9** shows a single resonance at 73.0 ppm. The same complex **5** was obtained by Kühl et al. in the reaction of $Mo(CO)_4(NCEt)_2$ with **1** [2c].

The reaction of ligand **2** with equimolar quantity of $Mo(CO)_6$ afforded a mixture of *cis*-$[Mo(CO)_4\{Ph_2PN(H)C_6H_{11}\}_2]$ (**6**) and *trans*-$[Mo(CO)_4\{Ph_2PN(H)C_6H_{11}\}_2]$ (**10**) in 20 and 29% yields, respectively. The IR spectrum of the *trans* isomer shows a single band in the carbonyl region at 1884 cm^{-1} and the ^{31}P-NMR spectrum shows a single resonance at 85.2 ppm with a coordination shift of 49.1 ppm. Further the structure of complex **10** was established by single crystal X-ray diffraction studies. The ORTEP diagram of complex **10** is shown in Fig. 2 and the crystallographic data and the selected bond distances and angles are listed in Tables 1 and 3, respectively. The molecule adopts a regular octahedral geometry around molybdenum with all *trans* angles being 180°, whereas the *cis* angles vary from 87.8 to 92.2°. The P–N bond distance of 1.679 Å is within the range of 1.66–170 Å expected for compounds with P–N multiple bonding. The Mo–P bond distance of 2.462 Å is slightly shorter than that in *trans*-$[Mo(CO)_4(PPh_3)_2]$ (2.500 Å) [23], *trans*-$[Mo(CO)_4$-

Table 2
Selected bond distances (Å) and bond angles (°) for **7**

Bond distances (Å)			
W(1)–P(1)	2.493(1)	W(2)–P(3)	2.496(1)
W(1)–P(2)	2.499(1)	W(2)–P(4)	2.488(1)
W(1)–C(1)	2.004(3)	W(2)–C(41)	2.011(3)
W(1)–C(2)	2.001(3)	W(2)–C(42)	2.007(3)
W(1)–C(3)	2.041(3)	W(2)–C(43)	2.030(3)
W(1)–C(4)	2.025(3)	W(2)–C(44)	2.040(3)
P(1)–N(1)	1.687(3)	P(3)–N(3)	1.699(3)
P(2)–N(2)	1.691(3)	P(4)–N(4)	1.690(3)
Bond angles (°)			
P(1)–W(1)–P(2)	90.70(2)	P(3)–W(2)–P(4)	89.9(2)
P(1)–W(1)–C(1)	89.6(1)	P(3)–W(2)–C(41)	91.3(1)
P(1)–W(1)–C(2)	174.8(1)	P(3)–W(2)–C(42)	174.6(1)
P(1)–W(1)–C(3)	94.1(1)	P(3)–W(2)–C(43)	93.0(1)
P(1)–W(1)–C(4)	85.8(1)	P(3)–W(2)–C(44)	85.7(1)
P(2)–W(1)–C(1)	175.8(9)	P(4)–W(2)–C(41)	176.0(1)
P(2)–W(1)–C(2)	90.1(1)	P(4)–W(2)–C(42)	87.3(1)
P(2)–W(1)–C(3)	86.2(1)	P(4)–W(2)–C(43)	87.7(1)
P(2)–W(1)–C(4)	93.5(1)	P(4)–W(2)–C(44)	94.6(1)
C(1)–W(1)–C(2)	90.0(1)	C(41)–W(2)–C(42)	91.8(1)
C(1)–W(1)–C(3)	89.6(1)	C(41)–W(2)–C(43)	88.4(1)
C(1)–W(1)–C(4)	90.6(1)	C(41)–W(2)–C(44)	89.3(1)
C(2)–W(1)–C(3)	91.1(1)	C(42)–W(2)–C(43)	91.6(1)
C(2)–W(1)–C(4)	89.0(1)	C(42)–W(2)–C(44)	89.8(1)
C(3)–W(1)–C(4)	179.7(1)	C(43)–W(2)–C(44)	177.7(1)

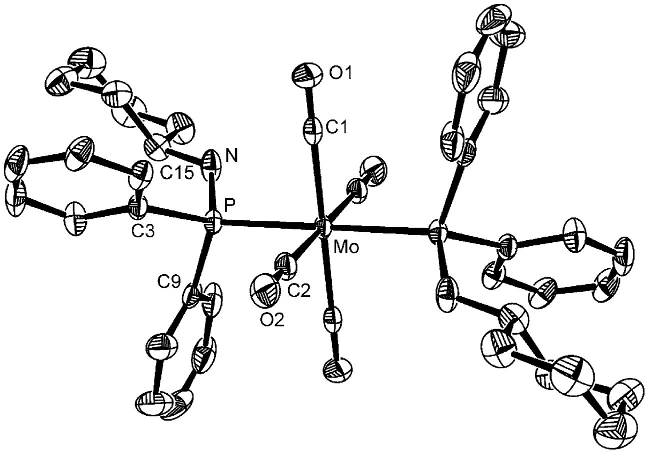

Fig. 2. ORTEP diagram of complex **10** (50% probability ellipsoids). Hydrogen atoms are omitted for clarity.

$(PhPC_4Me_4)_2]$ (2.480 Å), [24] and *trans*-$[Mo(CO)_4(PCy_3)_2]$ (2.544 Å) [25].

Interestingly, the reaction of ligand **2** with either $RuCl_2(DMSO)_4$ or $RuCl_2(PPh_3)_3$ in 4:1 molar ratio yielded the ionic complex, $[RuCl\{Ph_2PN(H)C_6H_{11}\}_3]Cl$ (**11**). The ^{31}P-NMR spectrum of complex **11** shows a single resonance at 76.4 ppm indicating the tetrahedral nature of the molecule and the mass spectrum of the complex shows a molecular ion peak corresponding to the cationic species. The rare low-coordination of ruthenium in the molecule is attributed to the sterically demanding aminophosphine ligands. However, a trigonal bipyramidal geometry around the ruthenium(II) center with two chlorides in axial positions and the three phosphorus centers in the trigonal plane can not be ruled out as the ^{31}P-NMR spectrum will show a single resonance.

Table 3
Selected bond distances (Å) and bond angles (°) for **10**

Bond distances (Å)			
Mo–P	2.462(1)	Mo–C(1)	2.039(3)
Mo–C(2)	2.046(3)	P–N	1.679(3)
P–C(3)	1.836(3)	P–C(9)	1.826(3)
N–C(15)	1.461(4)		
Bond angles (°)			
P–Mo–C(1)	90.7(1)	P–Mo–C(2)	92.2(1)
P–Mo–P(_a)	180.0	P–Mo–C(1_a)	89.3(1)
P–Mo–C(2_a)	87.8(1)	C(1)–Mo–C(2)	90.2(1)
P(_a)–Mo–C(1)	89.3(1)	P(_a)–Mo–C(2)	87.8(1)
C(1)–Mo–C(1_a)	180.0	C(1)–Mo–C(2_a)	89.8(1)
C(1_a)–Mo–C(2)	89.8(1)	C(2)–Mo–C(2_a)	180.0
P(_a)–Mo–C(1_a)	90.7(1)	P(_a)–Mo–C(2_a)	92.2(1)
C(1_a)–Mo–C(2_a)	90.2(1)		

The reaction of **1** with $Pd(COD)Cl_2$ resulted in the formation of chloro bridged dinuclear complex, $[Pd(\mu\text{-}Cl)(PPh_2O)(PPh_2OH)]_2$ (**12**) through the P–N bond cleavage. The ^{31}P-NMR spectrum of the complex shows a single resonance at 79.0 ppm. The absence of ν_{NH} in the IR and the N–Ph protons in the ^{1}H-NMR spectrum indicates the P–N bond cleavage. The reaction of K_2PdCl_4 with two equivalents of **1** in acetonitrile also leads to the formation of the same complex **12** in good yield. Dixon and Rattery have reported the formation of the same complex **12** in the reaction of K_2PdCl_4 with $Ph_2HP(O)/PPh_2Cl$ in water–acetone [26]. When the *cis*-$Cl_2Pd(PPh_2OCH_2)_2$-^{n}Bu_4calixarene was kept in chlorinated solvent it undergoes decomposition to give the same complex **12** [27]. The structure of complex **12** was confirmed by single crystal X-ray diffraction studies and the molecular structure (Figure S1 in Section 5) is similar to the one reported by Ghaffer et al. [28]. The reaction probably proceeds via the formation of the intermediate $PdCl_2(Ph_2POH)_2$ complex. The P–N bond cleavage takes place during coordination to form Ph_2POH which in turn forms the chloro bridged complex **12** as shown in Scheme 1.

The reaction of **1** with K_2PtCl_4 affords the platinum complex, $[Pt\{(PPh_2O)_2H\}_2]$ (**13**), via the cleavage in P–N bond. The ^{31}P-NMR spectrum of **13** shows a single resonance at 53.4 ppm with a $^{1}J_{PtP}$ coupling of 3958 Hz.

Reaction of ligands **1** and **2** with *cis*- $[PtCl_2(COD)]$ in dichloromethane in 2:1 molar ratio at r.t. afford *cis*-$[PtCl_2\{PPh_2N(H)R\}_2]$ (R = Ph, **14** and C_6H_{11}, **15**) in good yields. The ^{31}P-NMR spectra of complexes **14** and **15** show single resonances at 28.8 and 29.6 ppm with $^{1}J_{PtP}$ coupling of 3927 and 3951 Hz, respectively. The structure of the complex **14** has been established by single crystal X-ray diffraction studies and the perspec-

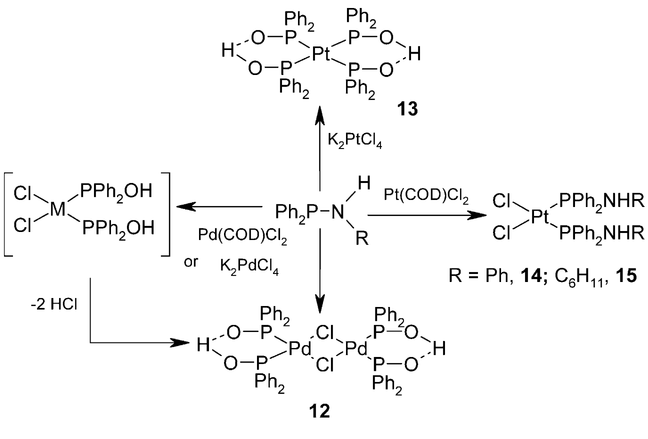

Scheme 1.

Table 4
Selected bond distances (Å) and bond angles (°) for **14**

Bond distances (Å)			
Pt(1)–Cl(1)	2.348(2)	Pt(2)–Cl(3)	2.254(2)
Pt(1)–Cl(2)	2.362(2)	Pt(2)–Cl(4)	2.353(2)
Pt(1)–P(1)	2.221(2)	Pt(2)–P(3)	2.253(2)
Pt(1)–P(2)	2.254(2)	Pt(2)–P(4)	2.239(2)
P(1)–N(1)	1.667(8)	P(3)–N(3)	1.634(8)
P(2)–N(2)	1.686(9)	P(4)–N(4)	1.669(8)
Bond angles (°)			
Cl(1)–Pt(1)–Cl(2)	86.6(1)	Cl(3)–Pt(2)–Cl(4)	86.6(1)
Cl(1)–Pt(1)–P(1)	84.4(1)	Cl(3)–Pt(2)–P(3)	87.6(1)
Cl(1)–Pt(1)–P(2)	170.0(1)	Cl(3)–Pt(2)–P(4)	174.1(1)
Cl(2)–Pt(1)–P(1)	170.7(1)	Cl(4)–Pt(2)–P(3)	172.7(1)
Cl(2)–Pt(1)–P(2)	86.9(1)	Cl(4)–Pt(2)–P(4)	90.8(1)
P(1)–Pt(1)–P(2)	102.3(1)	P(3)–Pt(2)–P(4)	95.4(1)

tive view of the molecule is shown in Fig. 3. The asymmetric unit contains two molecules but the corresponding bond distances and bond angles of two molecules are not significantly same as shown in Table 4. The platinum metal is in distorted square planar geometry and the angles around platinum vary from 84.4(1)° to 102.3(1)°. The average P–N bond distance (1.664(8) Å) is smaller than the sum of Pauling covalent radii (1.77 Å) as expected due to P–N multiple bonding. The average Pt–P bond distance (2.242(2) Å) in complex **14** is comparable with similar Pt(II) aminophosphine complexes such as, *cis*-[$PtCl_2\{Ph_2PN(CH_2Ph)CH_2CH_2(CH_2Ph)NPPh_2\}$] (2.241(3) Å) [8b], but longer when compared to the phosphinite complexes like, *cis*-[$PtCl_2\{PPh_2(OC_{10}H_6)(CH_2)$-$(OC_{10}H_6)PPh_2\}$] (2.226(3) Å) [8f] and shorter when compared to *cis*-[$PtCl_2(PMe_3)_2$] (2.315(10) Å) [29]. Complex **14** exhibits three different types of intermolecular hydrogen-bonding involving Cl and different phenyl hydrogens ($d_{C(27)\cdots Cl(3)} = 3.586(11)$ Å, $d_{H(27)\cdots Cl(3)} = 2.7131$ Å, C(27)–H(27)···Cl(3) bond angle = 153.12°; $d_{C(32)\cdots Cl(1)} =$ 3.399(11) Å, $d_{H(32)\cdots Cl(1)} = 2.5712$ Å, C(32)–H(32)···Cl(1) bond angle = 145.67°; $d_{C(54)\cdots Cl(4)} = 3.701(11)$ Å,

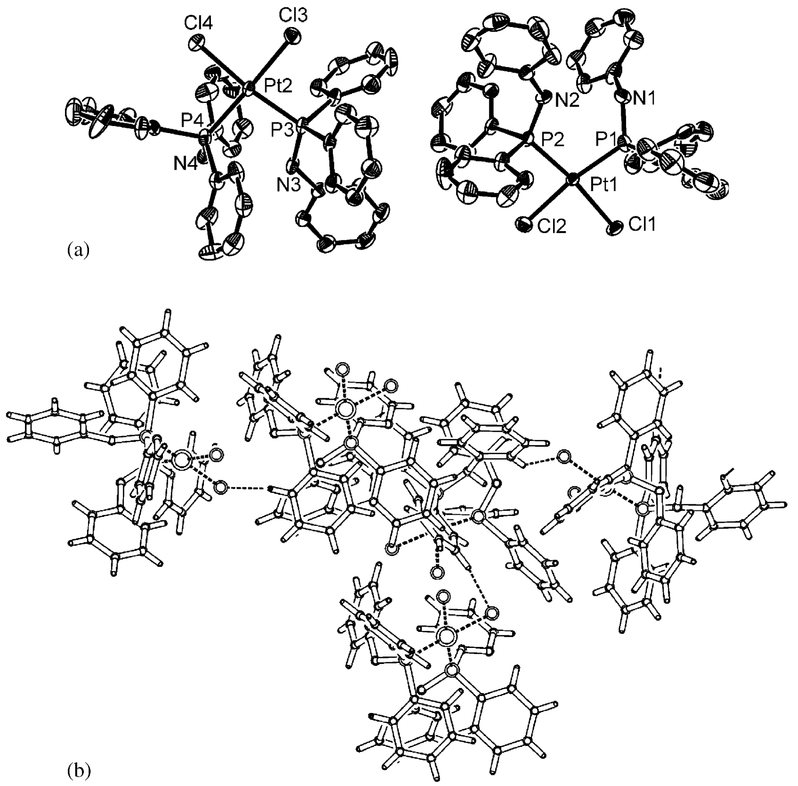

Fig. 3. (a) ORTEP diagram of complex **14**, ellipsoids are drawn on 50% probability level. Hydrogen atoms are omitted for clarity. (b) Cl···H–C intermolecular H bonding interactions.

$d_{H(54)\cdots Cl(4)} = 2.7699$ Å, C(54)–H(54)···Cl(4) bond angle = 166.69°) as shown in the Fig. 3(b).

The reaction of ligand **2** with the Ni(0) derivative, $Ni(CO)_2(PPh_3)_2$ in 2:1 molar ratio afforded *cis*-$[Ni(CO)_2\{PPh_2N(H)C_6H_{11}\}_2]$ (**16**) with the displacement of coordinated Ph_3P groups. The IR spectrum shows two bands for CO at 1997 and 1935 cm^{-1} indicating the presence of two CO groups. The ^{31}P-NMR spectrum shows single resonance at 22.2 ppm with the coordination shift of −13.9 ppm.

4. Conclusion

Several Group 6, ruthenium and Group 10 complexes of $Ph_2PN(H)R$ (R = Ph, C_6H_{11}) have been prepared. Molybdenum and tungsten complexes have been structurally characterized. The reactions of $Ph_2PN(H)R$ with $Pd(COD)Cl_2$ as well as K_2MCl_4 (M = Pd, Pt) leads to the cleavage of P–N bond and results in the formation of $[Pd(PPh_2O)(PPh_2OH)(\mu\text{-}Cl)]_2$ and $[Pt\{(PPh_2O)_2H\}_2]$. The reaction of $Ph_2PN(H)R$ with $Pt(COD)Cl_2$ gives the expected *cis*-$[PtCl_2(PPh_2N(H)R)_2]$ which has been structurally characterized. Both tungsten(0) and platinum(II) derivatives show intermolecular hydrogen-bonding interactions. The carbonyl complexes, $Ni(CO)_2(PPh_2N(H)R)_2$ and $M(CO)_4(PPh_2N(H)R)_2$ can be used as metallo-ligands for making heterobimetallic complexes with different by utilizing NH functionality. Similarly, the *cis*-dichloro platinum complex can act as a potential synthon to design high nuclearity clusters with the transition metals and the work in this direction is in progress in our laboratory.

5. Supplementary material

Full details of data collection and structure refinement have been deposited with the Cambridge Crystallographic Data Center, CCDC reference numbers 208304, 208306 and 208305 for compounds **7**, **10** and **14**, respectively. Copies of this information may be obtained free of charge from the Director, CCDC, 12 Union Road, Cambridge, CB2 1EZ, UK (Fax: +44-1223-336033; e-mail: deposit@ccdc.cam.ac.uk or www: http://www.ccdc.cam.ac.uk).

Acknowledgements

The Department of Science and Technology (DST) and the Council of Scientific and Industrial Research (CSIR), New Delhi, are acknowledged for the financial support of this work. SP is thankful to CSIR, New Delhi, for JRF and SRF fellowships. We thank the Department of Chemistry, Tulane University for the support of the Tulane Crystallography Laboratory. We also thank the Regional Sophisticated Instrumentation Center (RSIC), Bombay and Lucknow for NMR and mass spectra, respectively, and Sophisticated Instrumentation Facility (SIF) Bangalore, for NMR spectra.

References

[1] (a) M.S. Balakrishna, V. Sreenivasa Reddy, S.S. Krishnamurthy, J.F. Nixon, J.C.T.R. Burckett St. Laurent, Coord. Chem. Rev. 129 (1994) 1.;
(b) K. Raghuraman, S.S. Krishnamurthy, M. Nethaji, J. Organomet. Chem. 669 (2003) 79;
(c) K. Raghuraman, S.S. Krishnamurthy, M. Nethaji, J. Chem. Soc. Dalton Trans. (2002) 4289;
(d) S.K. Mandal, G.A.N. Gowda, S.S. Krishnamurthy, C. Zheng, S. Li, N.S. Hosmane, Eur. J. Inorg. Chem. (2002) 2047.

[2] (a) D. Fenske, B. Maczek, K. Maczek, Z. Anorg. Allg. Chem. 623 (1997) 1113;
(b) O. Kühl, P.C. Junk, E. Hey-Hawkins, Z. Anorg. Allg. Chem. 626 (2000) 1591;
(c) O. Kühl, S. Blaurock, J. Sieler, E. Hey-Hawkins, Polyhedron 20 (2001) 111;
(d) G. Suss-Fink, M.A. Pellingeelli, A. Tiripicchhio, J. Organomet. Chem. 320 (1987) 101.

[3] (a) A.D. Burrows, M.F. Mahon, M.T. Palmer, M. Varrone, Inorg. Chem. 41 (2002) 1695;
(b) M.S. Balakrishna, S.S. Krishnamurthy, Ind. J. Chem. 30A (1991) 536;
(c) M.G. Newton, R.B. King, M. Chang, J. Gimeno, J. Am. Chem. Soc. 100 (1978) 1632;
(d) J. Geicke, I.P. Lorenz, P. Murschel, K. Polborn, Z. Naturforsch. 52B (1997) 593.

[4] M.T. Ashby, Z. Li, Inorg. Chem. 31 (1992) 1321.

[5] F. Jakle, M. Mattner, T. Priermeier, M. Wagner, J. Organomet. Chem. 502 (1995) 123.

[6] O. Kühl, T. Koch, F.B. Somoza, P.C. Junk, E. Hey-Hawkins, D. Plat, M.S. Eisen, J. Organomet. Chem. 604 (2000) 116.

[7] (a) S. Priya, M.S. Balakrishna, J.T. Mague, Inorg. Chem. Commun. 4 (2001) 437;
(b) S. Priya, M.S. Balakrishna, J.T. Mague, S.M. Mobin, Inorg. Chem. 42 (2003) 1272.

[8] (a) M.S. Balakrishna, K. Ramaswamy, R.M. Abhyankar, J. Organomet. Chem. 560 (1998) 131;
(b) M.S. Balakrishna, R.M. Abhyankar, J.T. Mague, J. Chem. Soc. Dalton Trans. (1999) 1407;
(c) M.S. Balakrishna, R. Panda, J.T. Mague, Inorg. Chem. 40 (2001) 5620;
(d) M.S. Balakrishna, R.M. Abhyankar, M.G. Walawalker, Tetrahedron Lett. 42 (2001) 2733;
(e) M.S. Balakrishna, M.G. Walawalker, J. Organomet. Chem. 628 (2001) 76;
(f) M.S. Balakrishna, R. Panda, J.T. Mague, J. Chem. Soc. Dalton Trans. (2002) 4617.

[9] (a) P. Braunstein, M.D. Fryzuk, M.L. Dall, F. Naud, S.J. Rettig, F. Speiser, J. Chem. Soc. Dalton Trans. (2000) 1067;
(b) S.M. Aucott, A.M.Z. Slawin, J.D. Woollins, Polyhedron 22 (2003) 361;
(c) S.K. Mandal, G.A.N. Gowda, S.S. Krishnamurthy, M. Nethaji, J. Chem. Soc., Dalton Trans. (2003) 1016.

[10] W. Wiegrabe, H. Bock, Chem. Ber. 101 (1968) 1414.

[11] D. Drew, J.R. Doyle, Inorg. Synth. 13 (1972) 48.

[12] D.A. White, Inorg. Synth. 13 (1972) 52.

[13] P.R. Hoffman, K.G. Caulton, J. Am. Chem. Soc. 97 (1975) 4221.

[14] I.P. Evans, A. Spencer, G. Wilkinson, J. Chem. Soc. Dalton Trans. (1973) 204.

[15] R.B. King, Inorg. Chem. 2 (1963) 936.

[16] M.A. Bennett, L. Pratt, G. Wilkinson, J. Chem. Soc. (1961) 2037.

[17] D.J. Darensbourgh, R.L. Kump, Inorg. Chem. 17 (1978) 2680.

[18] K. Harms, S. Wocadlo, Program to Extract Intensity Data from Enraf-Nonius CAD-4 Files, University of Marburg, Marburg, Germany, 1987.

[19] M.C. Burla, M. Camalli, G. Cascarano, C. Giacovazzo, G. Polidori, D. Viterbo, Appl. Crystallogr. 22 (1989) 389.

[20] Bruker AXS, Madison, WI, 1995.

[21] J.T. Mague, C.L. Lloyd, Organometallics 7 (1988) 983.

[22] L.J. Farrugia, J. Appl. Cryst. 30 (1997) 565.

[23] G. Hogarth, T. Norman, Inorg. Chim. Acta 254 (1997) 167.

[24] K.W. Muir, F.Y. Pettilon, R. Rumin, P. Schollhammer, J. Talarmin, J. Organomet. Chem. 622 (2001) 297.

[25] E.C. Alyea, G. Ferguson, S. Kannan, Acta Crystallogr. C 52 (1996) 765.

[26] (a) K.R. Dixon, A.D. Rattery, Can. J. Chem. 49 (1971) 3997;
(b) K.R. Dixon, A.D. Rattray, Inorg. Chem. 16 (1977) 209.

[27] D.R. Evans, M. Huang, J.C. Fettinger, T.L. Williams, Inorg. Chem. 41 (2002) 5986.

[28] T. Ghaffer, A. Kieszkiewicz, S.C. Nyburg, A.W. Parkins, Acta Crystallogr. C50 (1994) 697.

[29] G.G. Messmer, E.L. Amma, J.A. Ibers, Inorg. Chem. 6 (1967) 725.